ELECTRONIC STRUCTURE OF AMORPHOUS INSULATORS AND PHOTOSTRUCTURAL EFFECTS IN CHALCOGENIDE GLASSES

D. A. DRABOLD, S. NAKHMANSON and X. ZHANG

Department of Physics and Astronomy,
Condensed Matter and Surface Science Program,
Ohio University, Athens, Ohio, 45701, USA
http://www.phy.ohiou.edu/~ drabold, drabold@ohio.edu

1. Introduction and Background

It is an exciting time to undertake theoretical studies of amorphous and glassy insulators. This is because theory and its prime tool, simulation, are reaching a level of realism necessary to explain many experimental observations and even to go beyond them in providing microscopic pictures of processes in disordered materials. In this paper we discuss the modeling of electronic structure and how this work may be developed to give qualitative insight into the localized-extended (Anderson) transition [1], a computationally and perhaps fundamentally valuable restatement of the electronic structure problem in terms of real-space localized (Wannier-like [2]) states, the impact of thermal fluctuations on electron states and transport, and the atomic-dynamical consequences of light exposure for photo-sensitive glasses.

The presence of disorder makes these systems particularly susceptible to perturbations. Two examples we will emphasize are lattice vibrations (which induce substantial temperature dependence in the energies and structure of band-tail states and transport), and light-induced effects. The latter is an open field in which phenomenological models have been proposed, and local microscopic models have been advanced. None of this work has been well justified yet with detailed atomistic calculations.

In our experience with a-Si and glasses, it emerges that a high degree of localization *implies* a strong electron-phonon coupling. It follows that light-induced occupation changes in such well localized states may lead to major photo-structural rearrangements. Thus, even static calculations of the structure of tail and defect states indicate the likely places in the network where lattice vibrations will strongly influence the electron energies and states and also reveal likely sites for photo-structural rearrangements.

It is fair to add that, while this is a time of great possibilities, there are several difficult theoretical problems to be handled in the interim. Ideal simulations would 1) produce accurate estimates of excited states, 2) properly track excited state dynamics (eg, post Born-Oppenheimer dynamics) and for the case of photo-structural studies, 3) provide explicitly for an external electromagnetic field (eg light) to properly handle photo-induced electronic transitions. In each case there are currently important approximations in place which could be improved. Preliminary work is quite encouraging, since even comparatively "simple" *ab initio* methods appear able to capture much of the physics.

2. What is a good model?

Before one can justify a theoretical study of electronic states in any disordered insulator, one must define the necessary attributes of a satisfactory atomistic model. It is common to see new models of disordered systems proposed which are structurally appealing, but otherwise untested. This is a misleading practice since it is also clear that a diverse variety of mutually inconsistent models can have a respectable X-ray or neutron static structure factor $S(Q)$. In particular, such diffraction measurements are obviously a *necessary but not sufficient* test for a structural model. It is clear from the nature of the diffraction measurement that the information extracted involves an average over a very large number of configurations.

On the other hand, electronic, optical or transport properties of a material depend on the nature of the electron states near the Fermi level which are well localized if in the gap. For understanding these properties, it is a requirement that the electron states near the gap are realistic. The defect states provide a valuable "window" into topological and/or chemical irregularities in the network, and thus provide specific, detailed information about the *atypical* features of the material. It is exactly these *defects* which normally determine photo-response, transport and doping properties of materials. So, even though the integrated spectral weight of these defect signatures might be tiny in a diffraction measurement, it is important for many purposes to be sure that the defects are properly represented in models. Spectroscopists have done a superb job of characterizing these defects through a variety of probes; theorists need to play a bit of "catch up" here for generating models with *realistic* defects.

The most common shortcoming of molecular dynamics (MD) generated models in the literature (including most from *ab initio* MD) is to have so many defects leading to states in the optical gap that the system is in fact closer to a poor metal than an insulating glass. The presence of a large number of defects in close proximity in energy and real space (inevitable in a small supercell model) implies de-localization of the defect wave functions. This is expected from a simple tight-binding argument (overlapping, resonant wave functions form de-localized bands, much like the case for impurity bands). This un-

physical de-localization then impacts any calculation of transport (as seen for example from the Kubo formula [3]) or photo-structural change (since light-induced occupation changes would have little effect if the states with occupation changes was spread over a large number of atoms). It is not even obvious that structural and dynamical characteristics of such a model are reliable. This is because some of the artificially extended defect states are *occupied*. As such, they influence the density matrix and therefore Hellmann-Feynman [4] forces, and consequently the equilibrium conformation of the model. In summary a model should not be accepted as describing an amorphous insulator until it passes the structural *and* electronic tests.

For studies of a-Si presented here, we exclusively use the models of DTW [5] which agree to an impressive degree with *all* experiments (structural, optical/electronic and vibrational). In section 7 we discuss a model of a-Se built with judicious use of *a priori* information about the qualitative (chainlike) topology of the material *and ab initio* MD. We discuss this point in detail in Ref. [6].

3. Model building: interatomic potential, simulation regime and *a priori* information

It is sometimes implied that employing the "best" Hamiltonian (eg most realistic interatomic interaction) leads automatically to the best structural model. The work of Djordjevic, Thorpe and Wooten [5] and Mousseau and Barkema [7] has made it clear that a thoughtful program of annealing and thoroughly probing configuration space is more important than having the most accurate Hamiltonian. In particular, a simple Keating [8] potential leads to the most realistic (that is, agreeing with all the experiments) models of a-Si in existence in large part because the scheme constrains the final model to be four-coordinated, as strongly suggested by experiments. No cell formed with empirical or *ab initio* MD is as accurate for electronic structure simply because the *a priori* information about four-coordination is not externally imposed (and MD cannot work this out for itself in part because of short time scales). Also, accurate *ab initio* methods are typically unable to directly provide a model as large as 1000 atoms, which is necessary for some studies (particularly of band tail states). Presumably an ideal approach would be to merge intelligent schemes like those of Refs. [5, 7] with an accurate first principles interatomic interaction. Such calculations would be very computer intensive, but are worth attempting, especially for complex systems like ternary chalcogenide glasses.

As a further piece of evidence supporting these points, the experimental work on polyamorphism [9] demonstrates that there can be *multiple* amorphous phases, just as there are often many crystalline polymorphs; it often happens that care is needed to start in some sense "near" the desired amorphous phase. This is *not necessarily* just an equilibrated liquid, especially for systems that are not glass formers.Thus, for a-Si, a direct quench from the melt

yields a dip in the electronic density of states instead of a state-free optical gap. The origin of this trouble is easy to ascertain: the liquid (a prediminantly six-fold *metal* [10]) is topologically quite distinct from amorphous (or crystalline) Si, and any rapid quench is certain to freeze in too many remnants of the liquid (such as overcoordination defects, which are more common than dangling bonds in most published MD quench simulations). Because of the qualitative difference in liquid and amorphous topology, it is perhaps not surprising that a-Si cannot be formed from a quench from the melt experimentally.

4. Calculations of electron states

Several different schemes are available to compute the electronic states in amorphous and glassy materials. Tight-binding Hamiltonians are often employed for this purpose [11]. For the case of elemental Si there are several reasonable choices available. For multinary materials it is difficult to obtain a simple tight-binding Hamiltonian which correctly describes the energetics of a wide variety of conformations.

First principles methods are becoming favored for these calculations because of transferability, and a local basis approach is recommended for three reasons: 1) the basis is sufficiently small that exact diagonalization is possible. This is important because eigenvectors of the Hamiltonian are sometimes needed, rather than linear combinations of eigenstates from the occupied subspace, which is the outcome of an (iterative minimization) planewave calculation. 2) Dynamics derived from "exact diagonalization" are exactly on the Born-Oppenheimer [12] surface, unlike the situation for Car-Parrinello [13] dynamics (for small-gap systems). Finally, 3) The "chemistry" is more easily interpreted with a local basis, so that the concepts of bonding, s and p character, etc. are all available. Current local basis codes like SIESTA [14] and FIREBALL2000 [15] enable state of the art accuracy within the general class of density functional methods.

5. Structure of electron states in a-Si. Zero temperature

5.1. DEEP DEFECTS

It is now clear that the midgap defect state is due to dangling bonds. The floating bond conjecture (that five-fold coordinated atoms play an important role in a-Si) has not been disproven, though it is clear that any such states are shifted well toward the conduction band edge [16] and are not nearly so localized as the sp^3 dangling bonds. If such floating bond defects exist, they might form resonances with the conduction tail states, which could have interesting implications for transport in n-type materials.

5.2. LOCAL SPIN DENSITY VERSUS LOCAL CHARGE DENSITY

For quantitative studies of localization (to compare the localization of a dangling bond defect electron state from an ESR experiment to theory) we have shown recently that the local spin density approximation (LSDA) is *required* [16]. Naively, this might be guessed since it is, after all, the unpaired *spins* which are measured in an ESR experiment, rather than the *charge*, which is readily extracted from any local density (LDA) calculation. The interesting point is that according to the accurate code SIESTA [14], there is a qualitative difference in the numerical value of the localization as computed from spin and charge densities. In particular, the LSDA gives a much better (more localized) result than the LDA, as compared to ESR in reasonable agreement with experiment. We also showed that the dominant optical gap deep defect of tetrahedral amorphous carbon (ta-C) [17] is π-bonded pairs with energies near the Fermi level, and these probably are responsible for the known ESR signal in this material, rather than classic sp^3 dangling bonds. More work is warranted on these essentially empirical observations.

5.3. BAND-TAIL STATES AND ANDERSON TRANSITION

We have discussed the details of the computation of gap and band tail states in the 4096 atom model of amorphous Si [5] elsewhere [18]; here I dwell upon the "physics" of the calculation. In a nutshell, we found that (1) states near the middle of the gap were exponentially localized (as one would expect); (2) for energies shifted from midgap toward the valence tail, there was a tendency to find system eigenstates with rather similar charge densities, and consisting roughly of two separated "blobs" of charge; (3) deeper into the valence tail we observed that the states still were discernibly "built" from clumps or clusters of charge, with a clear separation between these clumps; (4) deep into the valence tail we saw states that were well extended, essentially uniformly, through the cell. A color version of these states is given in Ref. [18] and the world wide web.

The preceding discussion suggests that an alternate basis or representation may be desirable to describe the electron states of a-Si, in the vicinity of the gap. As always in quantum mechanics, one is at liberty to select any complete (or at least approximately complete) set to represent the quantum mechanical states. The choice is normally made on grounds of efficiency: basis functions are selected which capture much of the character of the eigenfunctions, so that a linear combination of a small number of basis functions is required to represent the eigenfunctions. The classic example is the method of orthogonalized plane waves in band theory [19]. Likewise here, since the eigenvectors in the gap and near the tails are clearly composed of "lumps" or clusters of charge, a basis consisting of such cluster states is appealing.

We take the view that the cluster states are localized eigenfunctions which arise from idealized isolated defects. To illustrate the point, select a simple,

local distortion, say a strained bond angle significantly removed from the distribution of bond angles in the system. Suppose further that the strain is large enough to make the state bound (eg. localized) with exponential tail. Then the state has both a well defined energy and well defined extent in real space. Such a situation certainly exists in a-Si provided that the defect is really isolated (in space) from resonant (like-energy) defects. From this point of view, the highly localized states near the middle of the gap arising from single defects in large cells are examples of especially spatially compact cluster states. If one considers "real" a-Si, then there is some (energy dependent) probability that the original defect overlaps another like energy "resonant" defect. Should this happen, the system eigenstates would be (less localized) *mixtures* of the cluster states. As one considers energies closer to the valence and conduction bands (in the band tail regions), it becomes difficult to compute the cluster states exactly, since the density of states increases (which implies that the number of cluster states is also greater) so that the probablity is large that the tails of resonant defects overlap. Note that the resonance condition does not require that the defects be structurally similar – only that their energies should be close.

Our qualitative picture of the local to extended transition in a-Si, based on these calculations is the following: As severe distortions are rare, clusters stemming from such distortions are probably isolated from each other and if isolated, are localized energy eigenstates. For less severe distortion (and energies nearer to either band tail rather than midgap), the probability of occurrence increases, and the size of associated clusters is also larger. Then the chance of finding another cluster of similar energy in the neighborhood increases. As the distortion becomes less severe, system eigenstates will consist of mixtures of many clusters. At some point, the clusters can always find "overlapping energy partners" and they mix to enable electronic connectivity. This state of affairs can be identified with the "mobility edge".

With the preceding introduction, it is natural to write down a simple "theory" utilizing these ideas. A reasonable form for this model is:

$$\hat{H} = \sum_{\alpha} E_{\alpha} |\alpha\rangle\langle\alpha| + \sum_{\alpha\beta(\alpha\neq\beta)} |\alpha\rangle\xi_{\alpha\beta}\langle\beta| \qquad (1)$$

where, basis state $|\alpha\rangle$ is a localized cluster (*which may involve many atoms*). In this representation, the basis functions are localized energy eigenstates with eigenvalue E_α of the Hamiltonian in the absence of other defects with which mixing occurs. E_α is determined by the distortion. In real amorphous solids, the cluster states may significantly overlap. $\xi_{\alpha\beta}$ represents the coupling between cluster $|\alpha\rangle$ and $|\beta\rangle$. In the spirit of Hückel theory [20], we can take: $\xi_{\alpha\beta} \sim (E_\alpha + E_\beta)S_{\alpha\beta}/2$ for $S_{\alpha\beta} = \langle\alpha|\beta\rangle$. Then, in first order perturbation theory, the formation of eigenstates of **H** from these clusters becomes obvious; the first order correction to the zeroth-order (cluster) state $|\alpha\rangle$ is $\sum_{\beta\neq\alpha}\Gamma_{\alpha\beta}|\beta\rangle$, where $\Gamma_{\alpha\beta} = (E_\alpha + E_\beta)S_{\beta\alpha}/2(E_\alpha - E_\beta)$. The strong mixing for small energy denominators ($E_\alpha \approx E_\beta$), and the role of the overlap is indicated. For reasons

that are apparent, we have called this the "resonant cluster proliferation" model of the Anderson transition [18].

Since the cluster basis states $|\alpha\rangle$ are not precisely known, no calculations have yet been attempted in this representation. It is however easy to imagine a calculation in which model cluster states are introduced with characteristic decay lengths; and the role of the amorphous net is largely encoded into $\xi_{\alpha\beta}$. Even in the absence of new explicit calculations, I believe that the "resonant cluster" model is useful to understanding the Anderson transition, and the role of thermal disorder in a topologically disordered network, as we describe later.

5.4. REAL-SPACE LOCALIZED REPRESENTATION FOR ELECTRONS: GENERALIZED WANNIER FUNCTIONS FOR AMORPHOUS SI

In the quantum theory of solids, a natural approach to studying the electronic structure is to compute in some suitable approximation the system electronic eigenstates. The eigenfunctions of the Hamiltonian operator have extent through the entire system. For crystals, Bloch's theorem enables one to perform small diagonalizations on a mesh of **k** points to completely characterize the electronic structure. This is, of course, an eminently successful approach for crystals. Since the 1930's it has also been known [21] that the electronic structure problem in insulators could also be formulated using orbitals which decay rapidly in real space. This *Wannier representation* has been an important tool even for crystalline systems. While all of these methods are in principle valid in metals, they have little computational utility since one can show that the resulting localized orbitals exhibit a power law decay in that case [22].

There is much to recommend the use of a Wannier representation in amorphous insulators. It is inconvenient computationally to work with the system eigenstates, since these are extended throughout the cell (except perhaps for a few with energies near spectral band edges). Such extended states require storage scaling as the square of the number of atoms, and to compute all the states is at best an N^3 (N is number of atoms) procedure. Also, we believe that it is of fundamental interest to compute well localized Wannier-like functions (or the one-particle density matrix) in amorphous insulators in order to gauge an upper bound to just *how local* quantum mechanics can be in these materials. This is relevant to physical questions like: "If we induce a perturbation at a given site, on what length scale can we expect the system to respond"?

Thanks to the work of Ordejón and coworkers [23], and others [24, 25, 26], there has been a renaissance of interest in real space localized representations for the electron states for practical calculations. Vanderbilt demonstrated that these localized functions are ideal for computing the surprisingly subtle electric polarization in the solid state [27] and also showed how to construct optimally localized Wannier functions for crystals [28] (with a computational costs scaling cubically with the number of atoms). Dr. Ordejón gives a thorough treatment of this work in his article elsewhere in this volume, and we refer the reader to his article for a proper review. The code SIESTA [14] includes a

full implementation of an order-N method within a self-consistent local basis density functional framework.

Here, we briefly summarize our projection method [2]. In this scheme, the single particle density operator (projector onto the occupied electronic energy subspace) is explicitly represented as a polynomial (Chebyshev) approximation of the Fermi distribution function:

$$\hat{\rho} \;=\; [e^{\,\beta(\hat{H}-\mu)} \;+1]^{-1}, \tag{2}$$

where $\hat{H}$ is the Hamiltonian operator, μ is the chemical potential and β is usually used as a gauge of the sharpness of the projection rather than as an inverse temperature. The utility of this operator is that it may be used to directly compute the projection onto the electronic occupied subspace without any diagonalization or other non-linear scaling computational techniques. By applying $\hat{\rho}$ to a set of suitable local functions and orthonormalizing the resultant projected orbitals, one can obtain a localized representation for the electronic states. Where atomistic simulation is concerned, these states, which reside wholly in the occupied electronic subspace, may then be used directly for energy and force calculations, or probably more fruitfully as useful input into variational [23, 29] approaches. We have drawn a polite veil over mountains of details in this discussion, which are completely discussed in Ref. [2,30].

Figure 1 shows one such orthonormalized projected Wannier-like function in the tetrahedrally coordinated amorphous Si model containing 4096 atoms. For these computations, we used the local-orbital LDA Hamiltonian of Sankey and Niklewski [31]. The atomic orbitals in this Hamiltonian are strictly set to zero outside a certain cutoff range (5.0 bohr radii for Si). Because of the complete fourfold coordination of the system, we could start with sp^3 bonding orbitals as initial functions which are bonding combinations of hybrid orbitals pointing in bond directions. Furthermore, we used fixed localization regions during the projection which contained all atoms within seven bond steps from the originating bond. These regions were then dynamically adjusted during the orthonormalization. (For the particular Wannier function shown, the final localization region contained 476 atoms.)

Figure 1 depicts the charge density of the resulting Wannier state within a plane defined by the two atoms which form the initial bond, and a third neighboring atom. The three atoms are indicated by small white crosses. The grey scale describes a logarithmic charge density plot with densities reaching from its maximum value near the center to black outside the localization region. Additionally, the figure contains contour lines of equal charge density where the density logarithm crosses an integer value. The thick black lines which are composed of many contour lines represent node lines at which the Wannier function changes sign. For a more informative color image clearly displaying the bond charge and its spatial decay, see Ref. [30,32].

We selected the Wannier state at a bond at atom 32 of the Djordjevic, Thorpe and Wooten cell [5]. This atom has an extremely distorted environment as can be seen from the position of the third atoms in the figure which

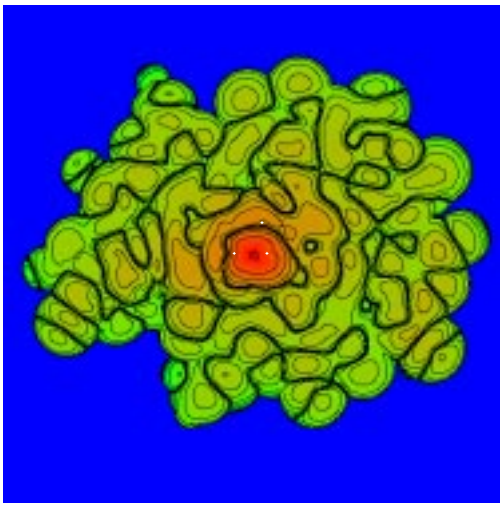

Figure 1. Orthonormalized Wannier function for amorphous Si as computed with the projection method of on 4096 atom model of amorphous Si and *ab initio* Hamiltonian. Solid black lines are "orthogonality nodes".

form a very small and a very large angle with the originating bond. These local distortions result in a sizable asymmetry of the Wannier-state in the immediate vicinity of the central bond. Nevertheless, the function is clearly localized and bonding at the originating bond, and is antibonding to the neighboring atom to fulfill the orthonormality constraint. When going out further in space, the function becomes highly irregular due to the disordered nature of the system. It oscillates several times until it reaches the boundary of the localization region. These boundaries are sharp in the logarithmic plot due to the cutoff in the atomic orbitals. However, a very interesting feature visible in Figure 1 is that the resulting Wannier functions are far from being spherical. This is a result we had already found earlier using a simpler Hamiltonian [2] The functions prefer to spread out in certain bond directions while they more quickly decay in other parts of their environment.

The overall radial decay of the Wannier state is shown in Figure 2. Here, we have plotted Mulliken's atomic gross populations (charge) of this state versus the distance from the bond center. The decay is approximately exponential especially in the maximum population values (dashed lines) which describe the

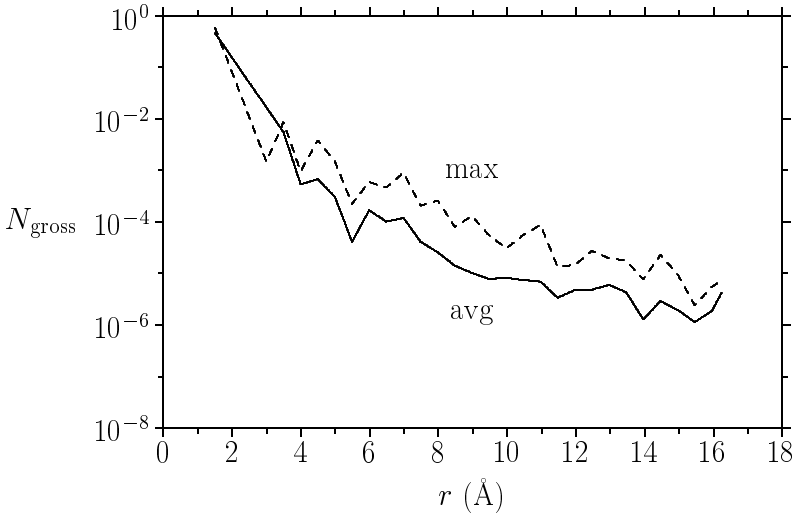

Figure 2. Decay of the Wannier functions in amorphous Si in real space as measured by Mulliken population.

envelope function. The decay becomes somewhat slower, however, at larger distances from the center. This effect is, at least to some extent, caused by the confinement of the Wannier states as we could show by similar computations in a smaller 512-atom amorphous Si model. An exponential decay is expected whenever the eigenstates which create the Wannier states (the occupied eigenstates in our case) are separated from the remaining (unoccupied) states by a gap. We have found by comparing our results to crystalline Si that the decay rates are surprisingly similar, suggesting that it is a *mobility* gap which determines the range of the density matrix and therefore the range of well-localized Wannier orbitals. However, there is not yet a completely general proof for this statement. Therefore, explicit computations of Wannier functions together with their tails also opens a way to a better understanding of the fundamental properties of these functions and the entire question of how best to formulate electronic structure calculations implemented in real space.

6. Structure of electron states. Finite temperature

There is abundant experimental evidence that lattice vibrations play an important role in the dynamics of electrons in amorphous materials [33]. Among other examples, Cohen and coworkers [34] observed a pronounced temperature dependence of the Urbach tails in a-Si:H (the conduction tails showing a very strong linear variation in exponential decay parameter with temperature). Of course electrical conductivity is well known to be very temperature de-

pendent, and usually has multiple distinct regimes according to different conduction mechanisms [35]. From this point of view it is unsurprising that the electron energies and states can be very time and temperature dependent. This point has been independently recognized by Arkhipov and Adriaennsens [36] in their studies of carrier transport. We build a microscopic picture of these effects in this section, beginning with a conventional discussion of electron-phonon coupling and the first explicit computation of this quantity. We then work beyond the harmonic approximation and study the development of electronic states as a consequence of a thermal MD simulation. We show that the electronic eigenvalues *and eigenvectors* can be profoundly sensitive to lattice vibrations. Our calculations have the advantage of being rather realistic, but the problem that they are restricted to very short (picosecond) time scales.

6.1. ELECTRON-PHONON COUPLING: *AB INITIO* DEFORMATION POTENTIAL

Earlier work has shown that it is useful to link the thermal fluctuation of the LDA energy eigenvalues near the band tails to the extent (localization) of the band tails in amorphous Si [37] (as separately measured in total yield photoemission experiments [34]). It is now routine in *ab initio* simulations to compute both the electronic and vibrational eigenvalues and eigenvectors. We show here that it is entirely straightforward to compute the electron-phonon coupling, a sort of "*ab initio* deformation potential" [38].

Consider a particular electronic eigenvalue, λ_n, say in one of the band tails in a-Si. To estimate the sensitivity of λ_n to a coordinate distortion (supposedly thermally induced), we can use the Hellmann-Feynman theorem [4], which gives $\partial\lambda_n/\partial\mathbf{R}_\alpha = \langle\psi_n|\partial\mathbf{H}/\partial\mathbf{R}_\alpha|\psi_n\rangle$ (for this to be valid, we must assume that the basis is fixed (not moving with the atoms) and that the $|\psi_n\rangle$ are exact eigenvectors of $\mathbf{H}$; see Ref. [31] for a more general case). Then clearly for small distortions $\delta\mathbf{R}_\alpha$, we have

$$\delta\lambda_n \approx \sum_\alpha \langle\psi_n|\partial\mathbf{H}/\partial\mathbf{R}_\alpha|\psi_n\rangle\delta\mathbf{R}_\alpha. \tag{3}$$

Here, $\mathbf{R}$ is the $3N$ vector of displacements for all of the atomic coordinates from equilibrium. If the displacements $\delta\mathbf{R}_\alpha(t)$ arise from classical vibrations, then one can also write:

$$\delta\mathbf{R}_\alpha(t) = \sum_\omega A(T,\omega)\ \cos[\omega t+\phi_\omega]\ \chi_\alpha(\omega), \tag{4}$$

where ω indexes the normal mode frequencies, $A(T,\omega)$ is the temperature dependent amplitude of the mode with frequency ω, ϕ_ω is an arbitrary phase, and $\chi_\alpha(\omega)$ is a normal mode with frequency ω and vibrational displacement index α. Using a temperature dependent squared amplitude $A^2(T,\omega) = k_BT/2M\omega^2$, it is easy to see that the trajectory (long time) average of the expression for $\delta\lambda_n^2$ is:

$$\langle \delta\lambda_n^2 \rangle \;\sim\; (k_B T/4M) \sum_{\omega} (\Xi(\omega)/\omega)^2, \tag{5}$$

where the electron[n]-lattice[ω] coupling $\Xi_n(\omega)$ is given by:

$$\Xi_n(\omega) \;=\; \sum_{\alpha} \langle \psi_n | \partial \mathbf{H}/\partial \mathbf{R}_\alpha | \psi_n \rangle \chi_\alpha(\omega). \tag{6}$$

It would be straightforward for a particular collection of vibrational states to include the correct Bose terms to obtain a result valid at low temperatures $T < \Theta_D$ (for Θ_D a salient Debye temperature). These expressions give a transparent expression for the thermally induced electron modulation as driven by the lattice-electron coupling $\Xi_n(\omega)$. If we follow Ref. [37] and make the coarse approximation of equating $\langle \delta\lambda_n^2 \rangle^{1/2}$ to the Urbach decay parameter [11], then this model would predict a square root dependence of the decay parameter with temperature, perhaps not easily distinguished from the linear dependence reported in Ref. [34].

It is easy to see why there is a correlation between an eigenstate's localization (as measured for example by inverse participation ratio) and its thermal rms fluctuation [39]. Note that $\Xi_n(\omega)$ will in general consist of a sum of many terms (for different α); the individual terms have no preferred sign, so that adding a large number of terms of comparable magnitude will lead to cancellation and a small sum. On the other hand, if only a very small number of terms are nonzero (as for the case when the electron state $|\psi_n\rangle$ is well localized), then there will be less cancellation and a larger contribution to the sum (and therefore to the fluctuation of the eigenvalue). This model is limited in many ways: it is classical, it is obviously strictly harmonic, and we are assuming no electronic level crossings or other departures from adiabatic (Born-Oppenheimer) dynamics [33]). Nevertheless, this simple model captures some of the right temperature dependent electronic effects observed and provides a useful new link to *ab initio* simulation methods.

The thermal effects on the electron *states* are more difficult to calculate with this approach, mostly because of problems with degeneracy if one tries to use perturbation theory. Still, the underlying "physics" is quite simple, just the effects of resonant mixing for close approach (in energy) of eigenvalues originating in cluster states with some overlap in space. In the language of the model Hamiltonian above, this means that there can be large mixing of cluster basis states when the energy denominator becomes small; here the thermal fluctuations can induce small energy denominators (and therefore mixing). Of course a mixed state involves more cluster states than a pure cluster state, so that it is more spatially extended.

We have explicitly computed $\Xi_n(\omega)$ for 216 atom models of a-Si [5] and a-Se [40]. We used the method of Sankey and coworkers for the interatomic potential [31] to compute the dynamical matrix [41] and estimated $\partial\lambda_n/\partial\mathbf{R}_\alpha$ from finite differencing λ_n for each of the 3N (small) displacements $\delta\mathbf{R}_\alpha$ needed for

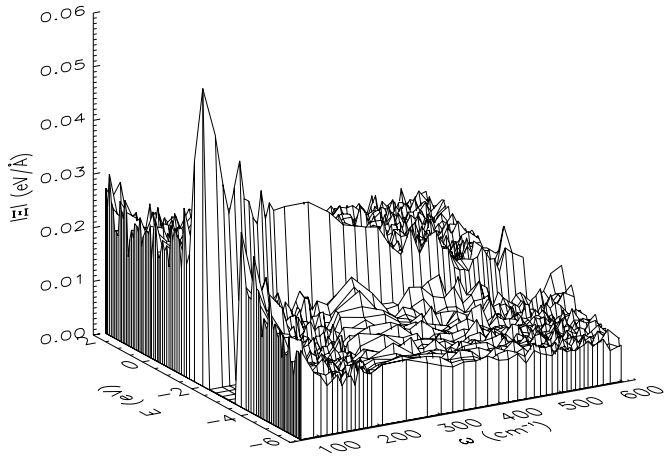

Figure 3. Electron-phonon coupling surface plot for 216 atom DTW model of amorphous Si. Phonon energy ω, electron energy *E* and absolute value of electron-phonon coupling Ξ (Equation 6). The optical gap extends from -3.45 to -2.11 eV. Note the dominance of *acoustic* phonons to the coupling. Compare to Fig. 5.

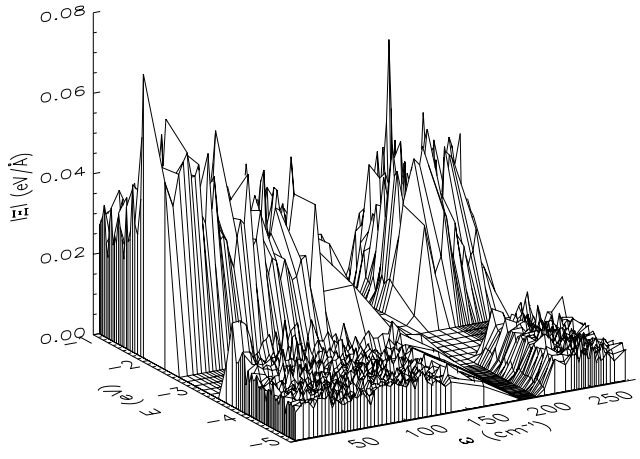

Figure 4. Electron-phonon coupling surface plot for 216 atom model of amorphous Se. Phonon energy ω, electron energy *E* and absolute value of electron-phonon coupling Ξ (Equation 6). The optical gap extends from -3.63 to -2.50 eV. In contrast to a-Si, optical phonons play an important role in the electron-phonon coupling in Se.

computing the dynamical matrix. $\Xi_n(\omega)$ is then easily obtained from Equation 6. Our results are summarized for a-Si in Figure 3 and for a-Se in Figure 4.

For the case of DTW a-Si there are no coordination defects, though there are a small number of strained structures which lead to a reasonable distribution of localized tail and gap states. Note that (1) the electron-phonon coupling is larger for conduction tail states than valence tail states (the conduction tails are also more localized), 2) the *acoustic* phonons are evidently more important to the tail states than optical phonons. This is also borne out by a dominant low frequency (eg acoustic) modulation of the tail electronic energies in the next section. 3) The electron-phonon coupling falls off rapidly for electron energies away from band edges.

The case of a-Se is largely similar except for one very interesting difference: the high energy "optical" phonons induce a large second "hump" in the surface plot (for phonon energies exceeding 200 cm^{-1}. In this model there is one valence alternation pair (threefold and onefold coordinated Se sites). It is possible that the spectacular photo-sensitivity of a-Se can be attributed in this framework to the simultaneous presence of localized electronic and vibrational modes *in the same region of space*, eg near the same defect. Note also that for a-Se, the conduction tail states (which derive mostly from positively charged threefold sites) are *much* better localized and exhibit a much larger electron-phonon coupling than the valence tail states. This large coupling is a primary reason for the photo-sensitivity of a-Se.

To directly estimate the fluctuations of the energy eigenvalues, we have evaluated Equation 5 for the cases of both a-Si and a-Se using the $\Xi_n(\omega)$ as presented in Figures 3 and 4 (see Figure 5). The floppy nature of the Se network, and the strong emphasis of Equation 5 on the *low frequency* phonons causes the RMS variation of the localized energy eigenvalues to be very large (of order 3.0 eV for room temperature); this is obviously too large, and a consequence of the large number of floppy modes and expected anharmonic character of a-Se. The results for a-Si are very reasonable, and in semiquantitative agreement with the discussion of the next subsection.

6.2. THERMAL MD SIMULATION

An alternative approach which avoids the harmonic approximation is to study the thermal modulation of the eigenvalues and eigenvectors by tracking their (adiabatic) time development over the course of a few picosecond (10^{-12}s) MD simulation. As illustrated in Figure 6, there is strong time dependence of the LDA eigenvalues in the vicinity of the optical gap. The Fermi level is near the middle of the gap and several states near the Fermi level are appropriately described as band tail states. These are much like the states which would be responsible for conduction in doped a-Si:H. As in earlier work [37] there is a roughly linear relation between root mean square (rms) temporal fluctuation and temperature. As expected, the higher temperature simulation leads to larger excursions in the positions of the energy eigenvalues. Note for 300K

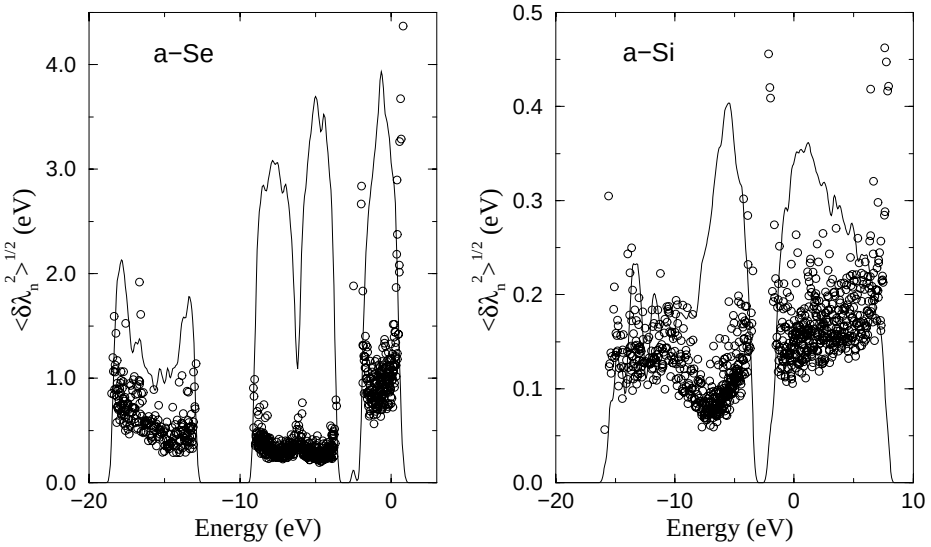

Figure 5. Crude estimates for RMS thermally-induced fluctuations in energy eigenvalues in the harmonic approximation from Equation 5 (open circles). Left is for a-Se model, right a-Si; note the difference in scales of the vertical axes. The relevant states are near the optical gap (near -2.5eV for Se, near -3.0 for Si). Note the large fluctuations in the conduction tail states for a-Se, which probably arise from anharmonic vibrations in the floppy a-Se network. The electronic density of states for each system is depicted with the solid line.

that the Lowest Unoccupied Molecular Orbital (LUMO) fluctuates in time by about $\sim$0.3eV, *much* larger than thermal energies ($\sim$10 meV). States deeper into either the valence or conduction bands show progressively less thermal modulation because they are less localized (we have noted [39] a very strong correlation between the rms fluctuation in the energy eigenvalues due to thermal disorder and the inverse participation ratio, a simple measure of localization in the T=0 model). The localization "amplifies" the electron-phonon coupling. Also, the conduction states fluctuate more than the valence states (suggesting that the conduction tails are more sensitive to thermal disorder than the valence tails which originate primarily from structural disorder), in pleasing agreement with total yield photoemission experiments [34] and earlier theory work [37]. We note that for a-Si, the harmonic approximation of the preceding section leads to semi-quantitative agreement with the RMS fluctuations computed directly from the thermal simulations of this section. For amorphous Se, it is clear that the harmonic computation *overestimates* the electron-phonon coupling, this is not very surprising for the highly floppy a-Se network.

An additional point is that these thermal simulations lead to low energy (acoustic) modulation of the localized electron states (especially for the conduction tail) in agreement with the discussion of the preceding section. The

importance of the low frequency vibrational modes is emphasized by the ω^{-2} factor in Equation 5, also consistent with the very large predicted RMS fluctuations in near-gap electron energies a-Se seen in the preceding section.

We have published color figures depicting the fluctuations in electron states near the gap for the system and dynamics described above. Here, for completeness, we give a monochrome figure (Figure 7) which conveys the same idea. There are very substantial changes in the LUMO state in particular; there is a clear tendency for the LUMO state to alternately "accumulate" on a strained part of the network, sometimes becoming localized, but also occasionally developing a substantially more extended "stringlike" character. These are not the only two recognizable structures, but recur most frequently. The time between "characters" is not predictable, though it is of order tens to hundreds of fs. We have posted an animation of this state on the world wide web [42].

We have argued in section 5.3 that structural disorder in a-Si gives rise to localized states with energies in the band tails. These system eigenstates can involve *many* atoms and can have a Byzantine [43] structure. The "simple physics" of this study is that the strong (compared to mid-band electrons) electron-phonon coupling for localized band tail states *is sufficient* to cause strongly time/temperature dependent quantum mechanical mixing of cluster states when the thermal disorder is "just right" to make their energies nearly degenerate provided that they have some overlap in real space. Strong mixing of course implies less localization and thus better prospects, at least while the more extended state survives, for conductivity and optical transitions. This work shows that transport and optical calculations based only on T=0 results can be quite misleading. Mott [35] and others have made fundamental contributions to the theory of transport in a noncrystalline medium; for example,variable range hopping. In the kind of simulation we present here, we can estimate the conductivity, including its temperature and frequency dependence *directly* from the electronic states through an appropriate thermal average of the Kubo formula [6]. It is also a complement to the phenomenological models of transport [36, 44]. In the latter work, transport is modeled as a hopping between localized tail states. Our work can be viewed as an explanation of the precise nature of the states among which electrons are hopping (the very complicated states of Ref. [18]). The waiting time between hops must be related to the time between eigenvalue "close encounters" near the Fermi level. It also points at an atomistic level to the dynamics of band tail defects and their kinetics.

The consequences of this work can be stated another way. If $|i\rangle$ ($|f\rangle$) are initial (final) electronic states with energy E_i (E_f), then for an electronic transition in a-Si, a Fermi golden rule argument leads quickly to the conclusion [35] that the transition rate is proportional to $|\langle i|\hat{T}|f\rangle|^2\delta(E_f - E_i - \hbar\omega)$, where $\hat{T}$ is a perturbation inducing the transition (to first approximation a momentum operator) and ω is the frequency of an external probe. Both the energies in the δ function and the transition matrix elements are affected by the instantaneous details of the structural disorder, and as such transition probabilities are also

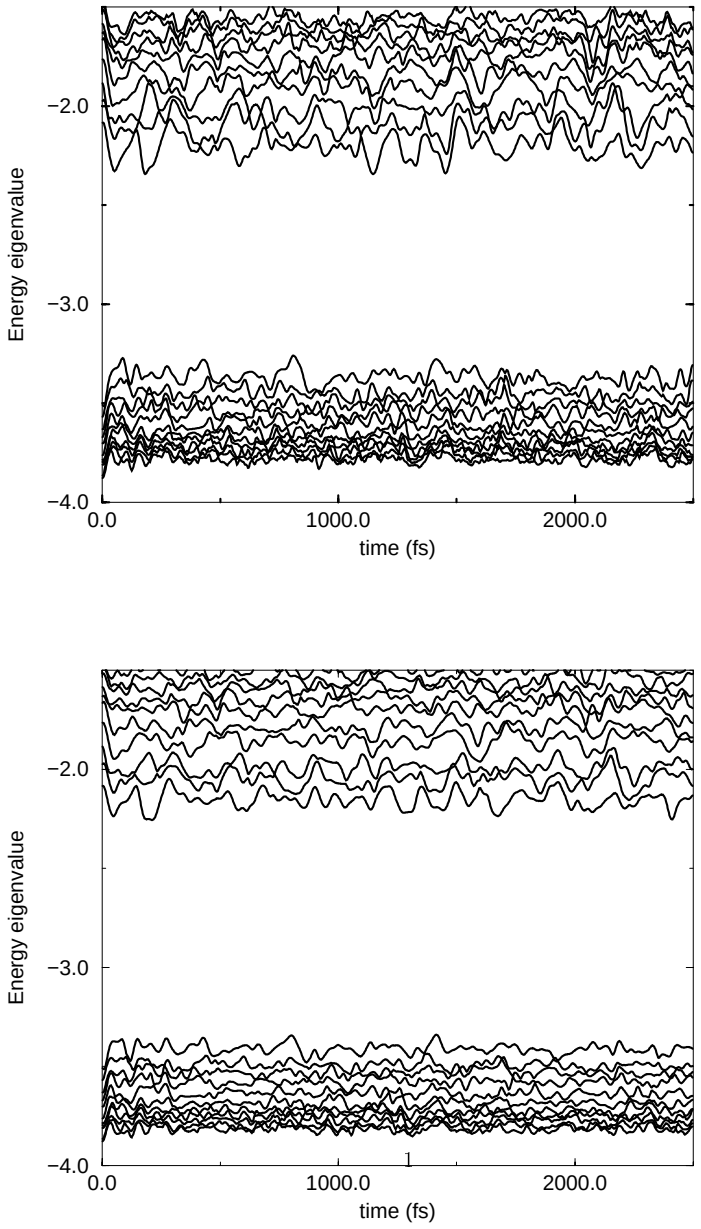

Figure 6. Adiabatic (Born-Oppenheimer) time evolution of LDA eigenvalues in 216 atom model of a-Si. Top panel 300K, bottom panel 150K. Note the larger fluctuations in conduction tail states compared to valence edge states. The Fermi level is near -2.7 eV. Compare to Fig. 3 and Fig. 5.

(a) A snaphot of the LUMO state:
time= 1147.5 fs

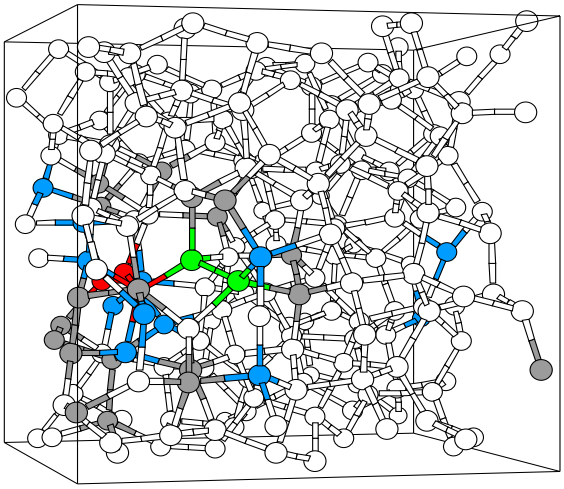

(b) A snaphot of the LUMO state:
time= 1032.5 fs

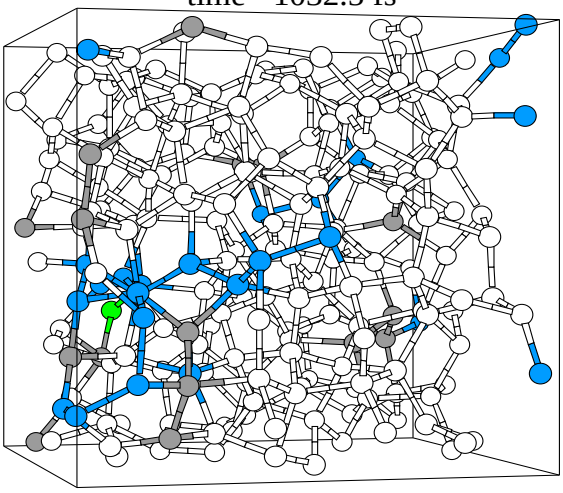

Figure 7. Time variation of the LUMO state in amorphous Si. The figure depicts the LUMO state at two different instants of time (separated by about 100fs).

strongly dependent on the time and temperature. The consequences of this to transport are under investigation; the discussion here is based upon first-order time dependent perturbation theory, which for the very strong electron-phonon coupling we discuss, could be inadequate.

6.3. POST ADIABATIC ATOMIC DYNAMICS – SPECULATIONS FOR FUTURE WORK

The calculations and discussion of the preceding sections has been based on the adiabatic approximation (that the electrons are always in their instantaneous ground state determined by the external potential (eg the atomic nuclei), and that the forces "felt" by the nuclei arose from the instantaneous electronic structure of the system.

To see that this might be an imperfect assumption, consider a doped system with a small concentration of dopants for which the Fermi level is pushed into one one of the band tails. Then the thermal modulation of the atomic coordinates may produce level crossings or close approaches of the LDA energies. In the doped case, there would normally be (occupied) levels below the Fermi energy and (unoccupied) levels above. In the case of a level crossing at the Fermi level, the adiabatic approximation would immediately transfer charge from one state to another (even if spatially remote), which would induce changes in the dynamics (since the levels with changed occupation would typically be at least somewhat localized); and perhaps could lead to a structural change, even a long lived change if the new structure was "self-trapping". In practical calculations such charge transfer would not have be quite so large an affect, since one would usually smear the Fermi function slightly from the $T = 0$ Heaviside step form. The dynamics are then affected by such level crossings or close approaches even in the adiabatic approximation. A better theory [45] is due to Allen, in which interatomic forces are computed from mixed state wave functions obtained by a direct integration of the *time-dependent* Schrödinger equation (rather than the "pure" states computed anew at each new time step for the atomic dynamics in the adiabatic picture). This approach was formulated to model the dynamical response of a system to light (in which the simplest model of light-solid interactions would just involve promotions of electrons to low-lying conduction states), but the formalism is similar (and much simpler) for the case of purely phonon-induced level crossings as in our problem. It is possible in fact that the adiabatic approximation may often be satisfactory for this kind of problem, but the question has not yet been properly investigated because of difficulties with post-adiabatic calculations. One case for which nonadiabatic dynamics is *essential* is in the modeling of the thermalization of excited carriers to tail states. This process has never been realistically modeled despite its manifest importance to a host of problems in crystalline and non-crystalline semiconductor physics. More sophisticated methods for non-adiabatic dynamics are discussed in the quantum chemistry literature [46]; while fundamentally sound, these are currently too difficult to

implement for the large model systems we must consider here.

7. Photo-structural effects

The basic goal of this section is to begin forging the connection between modern *ab initio* simulations and photo-induced properties of disordered systems. This is evidently a worthwhile project to attempt, since in principle these simulations provide everything needed (coordinates, dynamics, wave functions, etc). Much of the underlying thinking originates in our early attempt with Fedders and Fu to simulate the Staebler-Wronski effect in a-Si in 1992 [47]. We focus on a-Se here, since this system has a decidedly non-subtle response to light soaking, and we have an excellent atomistic model available.

7.1. A DYNAMICAL SIMULATION APPROACH TO PHOTO-STRUCTURAL EFFECTS IN GLASSES

In this section we outline a reasonable first attempt at modeling light-induced effects. We have applied the method to amorphous Se and glassy As_2Se_3. The first application of the method was to the Staebler-Wronski effect in amorphous Si [47].

Our simulation of photo-structural rearrangements is based upon the following reasoning:

- It is well known that topological or chemical irregularities in an amorphous network may lead to localized electron states in the gap or in the band tails.

- If such a system is exposed to band gap light, then it becomes possible for the light to induce transitions of electrons from the top of the occupied states to low-lying unoccupied (conduction) states. For the present model we will not concern ourselves with the subtleties of how the EM field introduces the transition; we will simply assume that a photo-induced promotion occurs. We discuss this problem further below.

- The key electronic "band structure" contribution to the interatomic force is

$$\mathbf{F}_\alpha = \sum_{n\ occ} \langle \psi_n | - \partial \mathbf{H} / \partial \mathbf{R}_\alpha | \psi_n \rangle, \tag{7}$$

  where the index implies that the sum is carried out over occupied states. Then the effect of the electronic promotion is to deplete the original set of occupied sttaes by one electron and add an electron to the unoccupied (conduction) states. If the light is exactly of bandgap energy, the electron will be promoted exactly from the top of the valence states to the bottom

of the conduction states. Thus, the change in forces for atom/Cartesian component index α is:

$$\delta \mathbf{F}_\alpha = \langle \psi_{N+1} | - \partial \mathbf{H} / \partial \mathbf{R}_\alpha | \psi_{N+1} \rangle - \langle \psi_N | - \partial \mathbf{H} / \partial \mathbf{R}_\alpha | \psi_N \rangle. \qquad (8)$$

Here ψ_{N+1} is the lowest unoccupied molecular orbital "LUMO" and ψ_N is the highest occupied molecular orbital "HOMO". There are in fact additional terms arising from charge transfer, but these are relatively simple to handle.

- The likelihood of a light induced structural change is then reduced in this model to the questions of whether $\delta \mathbf{F}_\alpha$ is large and if so, whether a new conformation becomes favorable. The key requirements are then that either or both of the states ψ_{N+1} or ψ_N are *well localized* and that the network admits the possibility of conformational change. If neither state is localized, then the change in forces from Equation 8 will be spread out over the volume in which the state extends. Thus, in crystals (where all the states are extended), occupation changes of the type we describe here never lead to changes. Similarly, in models with overly large defect concentrations, no changes are observed either (since the banding between defects (artificially) reduces the localization of the defect wave functions. Another statement (as from Section 6) is that a poorly localized wave function will have a small electron-lattice coupling with all the phonons, and no important photo-structural effects are to be expected for this case.

- In general, it is necessary to investigate photo-structural changes due to a collection of different initial and final states, though we may expect that only well localized states (necessarily near the gap) will be relevant.

We wish to apply these techniques rather generally to the rich field of photo-structural effects in glasses. This is by itself a broad area. Some of the most exciting effects are the opto-mechanical effect discovered by Krecmer *et al* [48], and photo-melting and related phenomena [49] as noted especially by Tanaka's group. As is usual in this area, there are several microscopic models proposed for these effects, which surely have much of the correct "physics" built in. Our work will give atomistic insight into the observations, enable studies of non-local behavior like photo-melting and ideally unravel incompletely understood processes like the optomechanical [48] effect.

It must be noted that the approach we suggest here is limited to *very* short (picosecond) time scales, and longer times and longer length scales require additional methods and study. Still, we believe that the approach presented here is an essential first step to understanding these problems as well.

7.2. PRACTICAL REALIZATION: AMORPHOUS SELENIUM

The unique photoelectronic properties of a-Se makes it an ideal material for photoreceptor in the photocopying process [50] and photoconductor in digital radiography [51]. Ample evidence that chalcogenide materials contain defect states derive from photoluminescence, photoconductivity, drift mobility and a pinned Fermi energy. But in contrast to amorphous column IV materials, there is no ESR signature of their presence. To explain this, Anderson [52] proposed a model in which a phonon coupling gives rise to a negative Hubbard energy U_{eff} to doubly occupy one-electron levels. An important extension of this idea by Street and Mott [53] argued that the negative U_{eff} in chalcogenides arises from lattice distortions at dangling-bond sites, which are unstable towards formation of charged defect centers with entirely paired spins. Subsequently, Kastner, Adler and Fritzsche [54] used simple chemical-bonding arguments to suggest that the lowest-energy neutral defect is a threefold-coordinated site which is unstable towards the creation of charged singly and threefold coordinated atoms, valence alternation pairs or VAP's.

Although the VAP model was successful in explaining most of the properties of lone-pair semiconductors, there has so far been no *realistic* calculation to support the existence of the negative U_{eff} and valence alternation in a-Se. The difficulty stems from two considerations. First, earlier calculations [55] imposed defects on Se chains which is taken to be the a-Se structure. Those artificial defects bear limited resemblance to real a-Se; Second, previous *ab initio* MD calculations [56] yielded too many coordination defects so that the defects cannot easily be analyzed as isolated entities. The defect-defect interaction causes an unphysical reduction in the localization of the defect wave function which affects interatomic forces and their sensitivity to occupation changes.

Here, we report the first *ab initio* study of light induced effects for a-Se. Our study of these important properties is made possible by use of *ab initio* MD in conjunction with a new algorithm for obtaining a model of a-Se. The resultant a-Se structure contains only one VAP defect and the structural properties including static structural properties S(Q), pair correlation function, electronic and vibrational density of states are in good agreement with experiment [57, 58]. Bond breaking and recombination of the structure due to optical excitation are directly simulated using this model. The signatures of photostructural change are in impressive agreement with the VAP model and recent experiment, though the process is less local than one usually imagines with the VAP model.

We used the program of Demkov, Ortega, Sankey and Grumbach [59] "Fireball96" to construct our network and use approximate Kohn-Sham orbitals as if they were "genuine" electron states. For the details of this method, the reader is referred to Refs. [59], [31]. The method has been used previously to form a small model of a-Se [60]. The use of Kohn-Sham states is not fundamentally justified, though there are many computations that show that this can

be useful [61]. Indeed, it is of some independent interest that these approximate and generously interpreted orbitals capture the physics quite well as we show below. We think this is because the effects we report here do not depend on particularly subtle features of the electronic structure.

Our approach to simulating a-Se involves two steps. We use a new algorithm to construct the amorphous structure for a large (216 atom) model. Realizing that the chain structure is the major component for a-Se, we build a long chain on a simple cubic lattice random walk as the initial configuration for our model. For our 216-atom model, we first obtained two chains with 199 atoms and 17 atoms as our initial model. The bond angle between two neighboring members of the chain is 90° and bond length is $2.15\mathring{A}$. Then, a standard *ab initio* MD "cook and quench" procedure was applied to this initial structure. It is quite interesting that a 159 atom ring, another ring with 25 atoms, a 24 atom chain starting on the 159 atom ring and ending unconnected, and one 5-atom ring appear in this 216 atom model. The chain is involved with both coordination defects (the unconnected end is of course one-fold, the connected end is three-fold). The appearance of 5-atom ring in this model gives additional strong evidence that coexisting long chains and rings is the basic structure of a-Se, as we also saw in our 64 atom calculation [60] This is in pleasing agreement with experiment [62].

To assess the validity of our 216 atom model a-Se structure, in Figure 8, we compare our computed pair distribution function $g(r)$, static structure factor $S(Q)$ and vibrational density of states with experiment where available. The calculated pair correlation function shows pleasing agreement with experiment [57] and peak positions agree closely with Ref. [63] and Ref. [64].

As shown in Figure 8(b), the static structure factor $S(Q)$ is in reasonable agreement with measurements taken from Ref. [57]. The location of principal peaks and intensities are close to the measured ones and even the oscillation between third and fourth peak in the experimental curve is exactly reproduced. The discrepancy in the first peak probably arises mostly from finite-size artifacts as we have tested in detail, though one cannot rule out that an extended exploration of configuration space might lead to closer coincidence. We stress however that the overall agreement is very satisfactory.

The vibrational density of states of a-Se has been studied using inelastic neutron scattering by Kamitakahara et al. [58]. and in Figure 8(c) we compare our VDOS with their experimental measurement. The agreement between the experiment and our simulation is excellent. Even the spectrum at the $20-30meV$ region is reproduced in our simulation. We will describe these modes elsewhere [65]. The lowest energy modes are extended.

We stress that our model is in *uniform* agreement with structural, vibrational and electronic measurements. For comparison, we also discuss light-induced effects in our earlier 64 atom model [60]. In our 64-atom model [60], there is only one "intimate" VAP (IVAP). The localized states at the top of the valence band arises almost soley from the singly coordinated sites. The localization at the conduction band edge is predominantly on the three-fold site and

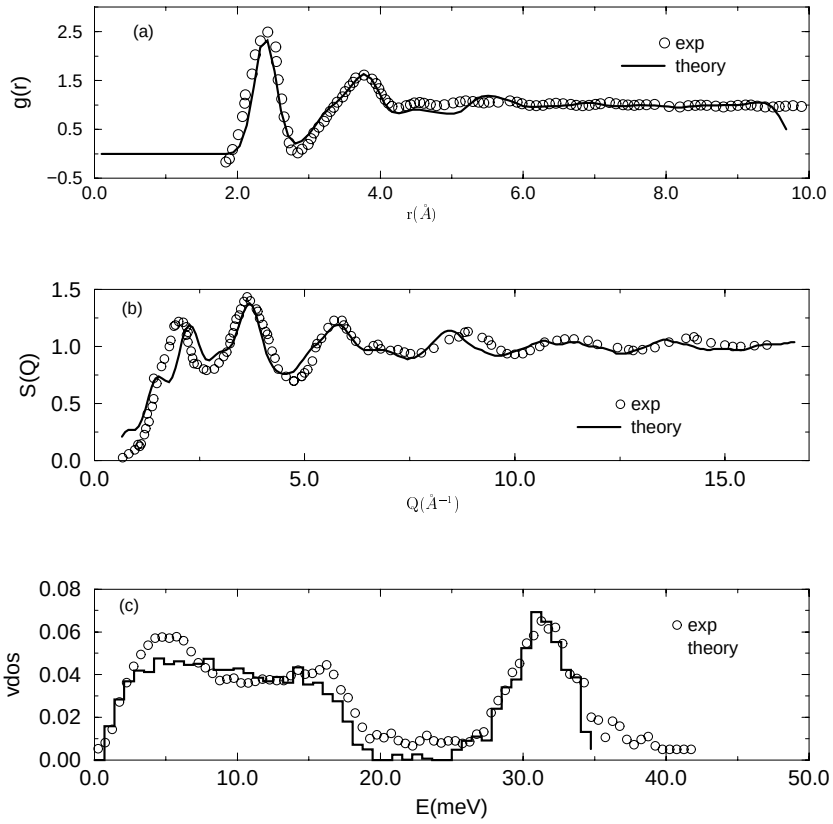

Figure 8. Model of amorphous Se, compared to experiment: a) pair correlation function, b) static structure factor, c) vibrational density of states.

its nearest neighbors. The important observation for IVAP defect in the 64-atom model is that the singly coordinated defect is more localized. This agrees with the early tight-binding calculation by Vanderbilt and Joannopoulos [55]. The density of electron states and the localization of defect eigenvectors of our 216-atom model [65] is similar to that of the 64-atom model [60].

The photostructural changes in chalcogenide glasses have been the subject of numerous investigations but the microscopic mechanism of such changes still remains unclear. If a model contains too many defects, it is hard to disentangle the structural change induced by optical excitation or other factors such as thermal disorder etc. Our models contain the fewest defect sites and as such, provide a suitable starting point for modeling the light-induced structural changes in a-Se.

We use the method developed by Fedders, Fu and Drabold [47] to simulate the light-induced structural change. First, we transfer the electron occupied at the HOMO to the LUMO level [66]. We imagine this change in the charge

of a localized state as a simple model of an electron ejected from the valence band to the conduction band by a photon. Then we let the system evolve freely without either adding or taking away energy. We found that the initial local disturbance of the atoms kept propagating outward. We let the supercell evolve for $400\,fs$ and observed how the topology changed during this optical excitation. Then we quenched the model to $T = 0K$. Other times ($200\,fs$ and $600\,fs$) were tested and the former led to no photostructural change, the latter to the same structure as $400\,fs$. A fuller study of this point is underway. We also repeated all this with constant temperature MD (300K) and found that the results were essentially identical.

Figures 9(a) and 9(b) reveal the structural change during this simulation for 64 atom model. We found that the one-coordinated defect was converted to a three-coordinated defect, and the structural change was somewhat non-local. Adjacent to the initial IVAP, two bonds were broken and two of the resulting defect atoms formed a new bond. One of the new defects converted to a three-coordinated defect and the other remained a one-coordinated defect. The fact that the original one-coordinated defect site was converted to the three-coordinated defect site is just another prediction by VAP model. Since the negatively charged one-coordinated defect atom become neutral C_1^0 by the optical excitation, this C_1^0 is not very stable and it tends to convert to C_3^0. The change in the other region is also easy to be understand if we assume the C_3^0 defect to be the most probable neutral defect in a-Se. *The local disturbance in the defect region will first cause bond breaking producing some C_1^0 defects, and these C_1^0 defects have a propensity to convert to C_3^0 defects.* Thus, it appears that the key to understand the structural change by optical excitation is to admit the assumption, C_3^0 being the most stable defect in a-Se. This is an important assumption in the VAP model by Kastner et al. [54]. We computed atomic charges using a Mulliken analysis and find that one-fold atoms are negatively charged (depending somewhat on the local environment, a charge of 0.07-0.1e is transferred); three-fold atoms are postively charged and by a similar amount. Two-coordinated sites have a typical charge of magnitude less than $\approx$ 0.02e. We performed tests with DMOL [67] and found semi quantitative agreement with fireball96 charges for a 17 atom Se molecule with an IVAP.

Fig. 10(a) and 10(b) shows the photostructural change for 216-atom model. As for the 64-atom model, the one-coordinated defect converts to a three-coordinated defect. A majority of photo-created defects are three coordinated suggesting that these are the most probable neutral defects in a-Se. It is interesting that three-coordinated defects tend to cluster together. This phenomenon was also observed in the calculation of Hohl et al. [56]

We have found that in both the 64 and 216 atom models, that the HOMO and LUMO levels move into the middle of the gap during the photoexcitation process. This is readily explained by the VAP model and the associated states are localized on miscoordinated neutral defects.

The final step is to de-excite the electron and then quench the sample. It is striking that all the defects disappear after we quench the system to an

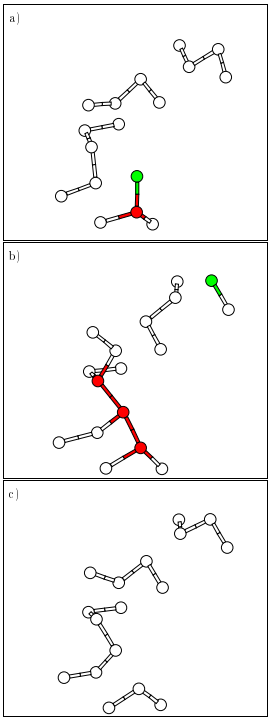

Figure 9. Photostructural rearrangements in 64 atom model of a-Se. Only active atoms are shown. Note that all defects are "photo-annealed" away in the final phase. Two-coordinated atoms: open circles, three-fold: solid black, one-fold: grey.

energy minimum for 64-atom model. This structural change is shown in Figure 9(c). This structural change then reveals one possible outcome, an interesting "optical annealing", rather akin to light-induced crystallization. For 216-atom model, as shown in Figure 10(c), the original VAP defect disappears and a new IVAP defect is formed.

We repeated the same MD simulations for the above processes without optical excitation. We use the same parameters, time step and quench rate except that we did not remove the electron from our system. After we let the system freely evolve for $400\,fs$ and quench it back. The structure is the same as the original structure. This indicates that the structural change in our first simulation is really induced by optical excitation.

Our structural model gives a description of the microscopic a-Se network of unprecedented quality, as evidenced by the comparison with experimental data where available. A recent generalized gradient approximation (GGA) calculation [68] gave a better agreement with experiment for l-Se. So, it is proposed by Kirchhoff et al. that GGA is essential to obtain the proper nearest-neighbor distance. We have verified that our Hamiltonian gives a dimer bond

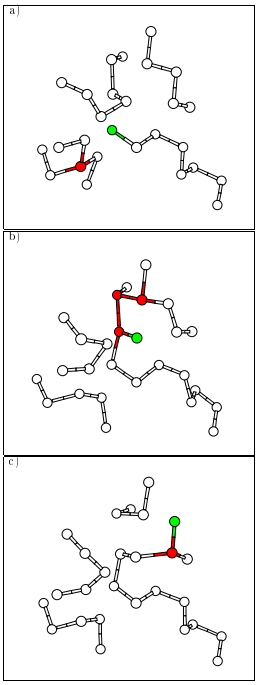

Figure 10. Photostructural rearrangements in 216 atom model of a-Se. Only active atoms are shown. In contrast to Fig. 9, the net effect of the photoexcitation is to induce defect diffusion. Labeling scheme as in Fig. 9.

length of 2.18$\mathring{A}$ which is close to experimental length 2.17$\mathring{A}$. We noticed that the improvement from GGA calculation by Kirchoff et al. is from decreasing the depth of the first minimum in the pair correlation function $g(r)$ which is much higher in the LDA calculation as well as in the Hohl and Jones calculation. To verify this point, we did two studies. First, we use a steepest descent quench to fully relax Hohl and Jones' network with our Hamiltonian [59]. The quenching decreases the first minimum of $g(r)$ and the resulting $g(r)$ is in improved agreement with experiment. The relaxed model only contains a bonded $C_3 + C_1$ IVAP pair and a pair of C_3 and C_1 (VAP). Second, we used the powerful first principles MD program, SIESTA, [14] to relax our 64-atom model. We included the GGA and pseudopotential core correction with a double-zeta polarized basis to quench our 64-atom model. However, we did not observe the improvement to the structural properties of our model by this more expensive calculation.

One additional implication of this work is that neutral C_3^0 is easy to form.

These C_3^0 defects may be frozen in the material if the system is quenched very quickly. This may explain why most of the theoretical calculation and some experiment showed that the coordination number for $a-Se$ is slightly larger than 2.

8. Conclusion

In this paper we have reviewed some of the interesting current activity in electronic structure calculations, especially as applied to amorphous and glassy materials. We wish to thank Jianjun Dong, Uwe Stephan, Normand Mousseau, Ron Cappelletti, Sergio Ulloa, Otto Sankey, Pablo Ordejón, Richard Martin, Peter Fedders, Mike Thorpe and Himanshu Jain for various contributions. This work was supported in part by the US NSF under grants 96-18789, 96-04921 and 00-81006.

References

1. P.W. Anderson, Phys. Rev. **109**, 1492 (1958).
2. U. Stephan and D. A. Drabold, Phys. Rev. B **57** (1998) 6391; U. Stephan, R. M. Martin and D. A. Drabold, *Extended range computation of Wannier functions in amorphous semiconductors*, Phys. Rev. B (in press). These ideas have also been explored in: S. Goedecker and L. Colombo, Phys. Rev. Lett. **73**, 122 (1994); O. F. Sankey, D. A. Drabold, and A. Gibson, Phys. Rev. B **50**, 1376 (1994).
3. D. J. Thouless, Phys. Rept. **13** 93 (1974).
4. R. P. Feynman, Phys. Rev. **56**(1939) 340; H. Hellmann, *Einfuhrung in die Quantumchemie* (Franz Deutsche, Leipzig, 1937)
5. B.R. Djordjevic *et al.*, Phys. Rev. B, **52**, 5685 (1995); F. Wooten and D. Weaire, Solid State Physics, edited by H. Ehrenreich and D. Turnbull (Academic Press, New York, 1991), Vol. 40, p.2
6. D. A. Drabold in *Insulating and Semiconducting glasses*, Edited by P. Boolchand, World Scientific, Singapore (2000).
7. G. T. Barkema and N. Mousseau, Phys. Rev. Lett. **77**, 4358 (1996); N. Mousseau and G. T. Barkema, Phys. Rev. E **57**, 2419 (1998), Comp. Sci. Eng. **1**, No. 2, 74 (1999), N. Mousseau and G. T. Barkema, Phys. Rev. B **61**, 1898-1906 (2000).
8. See for example, R. M. Martin, Phys. Rev. B **1** 4005 (1970).
9. For example, J. L. Yarger *et al Polyamorphic transitions in network-forming liquids and glasses*, ACS Symp. Series **676** 214 (1997).
10. G. Fabricius, E. Artacho, D. Sanchez-Portal, P. Ordejon, D. A. Drabold and J. M. Soler, Phys. Rev. B 60 R16283 (1999).
11. L. J. Lewis and N. Mousseau, Comp. Mater. Sci. **12** 210-241 (1998).
12. M. Born and K. Huang, *The dynamical theory of crystal lattices*, Oxford, Clarendon (1954).
13. R. Car and M. Parrinello, Phys. Rev. Lett. **55** 2471 (1985).
14. D. Sánchez-Portal, P. Ordejón, E. Artacho and J. M. Soler, Int. J. of Quantum Chem. **65**, 453 (1997).
15. J. Lewis, A. Demkov, J. Ortega and O. F. Sankey (unpublished).

16. P. A. Fedders, D. A. Drabold, P. Ordejón, G. Fabricius, D. Sanchez-Portal, E. Artacho and J. M. Soler, Phys. Rev. B **60** 10594 (1999).
17. D. A. Drabold, P. A. Fedders and P. Stumm, Phys. Rev. B **49** 16415 (1994).
18. Jianjun Dong and D. A. Drabold, Phys. Rev. Lett. **80** (1998) 1928.
19. C. Herring, Phys. Rev. **57** (1940) 1169.
20. W. Harrison, *Electronic Structure*, Freeman, San Francisco, (1980).
21. G. H. Wannier, Phys. Rev. **32** 191 (1937).
22. See for example the seminal work of Kohn: W. Kohn, Phys. Rev. **133** A171 (1964).
23. P. Ordejón, D. A. Drabold, M. P. Grumbach, and R. M. Martin, Phys. Rev. B **48**, 14 646 (1993); P. Ordejón, D. A. Drabold, R. M. Martin, and M. P. Grumbach, Phys. Rev. B **51**, 1456 (1995); F. Mauri, G. Galli, and R. Car, Phys. Rev. B **47**, 9973 (1993).
24. P. Ordejon, Comp. Mater. Sci. **12** 157-191 (1998).
25. S. Goedecker, Rev. Mod. Phys. **71** 1085-1123 (1999).
26. X.-P. Li, R. W. Nunes, and D. Vanderbilt, Phys. Rev. B **47**, 10 891 (1993); R. W. Nunes and D. Vanderbilt, *ibid.* **50**, 17 611 (1994).
27. See for example, R. W. Nunes and D. Vanderbilt, Phys. Rev. Lett. **73** 712 (1994).
28. N. Mazari and D. Vanderbilt, Phys. Rev. B **56** 12847 (1997).
29. U. Stephan, D. A. Drabold and R. M. Martin, Phys. Rev. B **58** 13472 (1998).
30. Various aspects of this work have been reported in: U. Stephan, D. A. Drabold and R. M. Martin, Phys. Rev. B (in press), and D. A. Drabold. U. Stephan, J. Dong and S. Nakhmanson, J. Mol. Graphics and Modelling (in press). The latter includes color images relevant to many points discussed in this article.
31. Otto F. Sankey, D.J. Niklewski, Phys. Rev. **B40**, 3979 (1989); Otto F. Sankey, D.A. Drabold and G.B. Adams, Bull. Am. Phys. Soc. **36**, 924 (1991).
32. http://www.phy.ohiou.edu/~drabold/cent.html
33. D. A. Drabold and P. A. Fedders, Phys. Rev. B **60** (1999) R721.
34. S. Aljishi, J. D. Cohen, and L. Ley, Phys. Rev. Lett. **64** (1990) 2811.
35. N. F. Mott and E. A. Davis, *Electronic processes in non-crystalline materials*, 2nd ed. (Clarendon, Oxford, 1979).
36. V. I. Arkhipov and G. J. Adriaenssens, J. Non-Cryst. Sol. **227** (1998) 166; Phys. Rev. B **54** (1996) 16696.
37. D. A. Drabold, P. A. Fedders, S. Klemm and O. F. Sankey, Phys. Rev. Lett. **67** (1991) 2179.
38. D. A. Drabold, J. Non.-Cryst. Sol. **266** 211 (2000).
39. M. Cobb and D. A. Drabold, Phys. Rev. B **56** (1997) 3054.
40. X. Zhang and D. A. Drabold, Phys. Rev. Lett. **83** 5042 (1999).
41. P. Ordejon, D. A. Drabold and R. M. Martin, Phys. Rev. Lett. **75** 1324 (1995).
42. For an mpeg format animation, see: http://www.phy.ohiou.edu/~drabold/fluctuate.html
43. E. Gibbon, *The Decline and Fall of the Roman Empire*, abridged edition by D. M. Low, (Harcourt Brace, New York, 1960).
44. See, for example P. Thomas and S. D. Baranovskii, J. Non-Cryst. Sol. **164**, (1996) 431 and references therein.
45. R. E. Allen, Phys. Rev. B **50** (1994) 18629.
46. See for example, K. Thompson and T. J. Martinez, J. Chem. Phys. **110** (1999) 1376 and references therein.
47. P. A. Fedders, Y. Fu and D. A. Drabold, Phys. Rev. Lett. **23** 1888(1992).
48. P. Krecmer, A. M. Moulin, R. J. Stephenson, T. Rayment, M. E. Welland and S. R. Elliott, Science **277** 1799 (1997).
49. H. Hisakuni and Ke. Tanaka, Science **270** 974 (1995).

50. J. Mort, Physics Today **47**, 32 (1994).
51. J. Rowlands and S. Kasap, Physics Today, **50**, 24 (1997).
52. P. W. Anderson, Phys. Rev. Lett. **34**, 953 (1975).
53. R.A. Street and N.F. Mott, Phys. Rev. Lett. **35**, 1293 (1975).
54. M. Kastner, D. Adler and H. Fritzsche, Phys. Rev. Lett. **37**, 1504 (1976).
55. D. Vanderbilt and J.D. Joannopoulos, Phys. Rev. **B22**, 2927 (1980).
56. D. Hohl and R.O. Jones, Phys. Rev. **B43** 3856, 1991.
57. R. Bellissent, Nucl. Instr. and Meth. **199**, 289 (1982).
58. W. A. Kamitakahara (private communication).
59. A.A. Demkov, J. Ortega, O.F. Sankey and M. Grumbach, Phys. Rev. **52**, 1618 (1995).
60. X. Zhang and D. A. Drabold, J. Non-Crystalline Solids **241**, 195 (1998).
61. F. Mauri and R. Car, Phys. Rev. Lett. **75** 3166 (1995); J. Song *et al*, phys. Rev. B **53** 8042 (1996); O. Pankratov and M. Scheffler, Phys. Rev. Lett. **71**, 2797 (1993); For transport, G. Galli *et al.* Phys. Rev. Lett. **42** 7470 (1990).
62. B. W. Corb , W. D. Wei and B. L. Averbach, J. Non-Crystalline Solids **53**, 29 (1982).
63. E.H. Henninger, R.C. Buschert and L. Heaton, J. Chem. Phys. **46**, 586 (1967).
64. R. Kaplow, T.A. Rowe and B.L. Averbach, Phys. Rev. **168**, 1068 (1968).
65. X. Zhang and D. A. Drabold, (unpublished).
66. We promoted either one or two electrons from the HOMO level; relaxations were similar. We report the two electron case here. The single electron promotion is probably best handled at LSDA level.
67. For example, B. Delley, "DMol, a Standard Tool for Density Functional Calculations: Review and Advances". In J. M. Seminario and P. Politzer, eds., "Modern Density Functional Theory: A Tool for Chemistry", vol. 2 of Theoretical and Computational Chemistry, Amsterdam, 1995. Elsevier Science Publ.
68. F. Kirchhoff, G. Kresse and M.J. Gillan, Phys. Rev. **B57**, 10482 (1998).